



Spin diffusion length associated with out-of-plane conductivity of Pt in spin pumping experiments

C. Gonzalez-Fuentes ^{*}, R. Henriquez, and C. García 

Departamento de Física, Universidad Técnica Federico Santa María, Avenida España 1680, 2390123 Valparaíso, Chile

R. K. Dumas

Quantum Design Inc., 10307 Pacific Center Court, San Diego, California 92121, USA

B. Bozzo and A. Pomar

Instituto de Ciencia de Materiales de Barcelona-Consejo Superior de Investigaciones Científicas, Bellaterra, Spain



(Received 14 September 2020; revised 18 March 2021; accepted 7 May 2021; published 1 June 2021; corrected 7 June 2021)

We present a broadband ferromagnetic resonance study of the Gilbert damping enhancement ($\Delta\alpha$) due to spin pumping in NiFe/Pt bilayers. The bilayers, which have negligible interfacial spin memory loss, are studied as a function of the Pt layer thickness (t_{Pt}) and temperature (100–293 K). Within the framework of diffusive spin pumping theory, we demonstrate that Dyakonov-Perel (DP) or Elliot-Yaffet (EY) spin relaxation mechanisms acting alone are incompatible with our observations. In contrast, if we consider that the relation between spin relaxation characteristic time (τ_s) and momentum relaxation characteristic time (τ_p) is determined by a superposition of DP and EY mechanisms, the qualitative and quantitative agreement with experimental results is excellent. Remarkably, we found that τ_p must be determined by the out-of-plane electrical resistivity (ρ) of the Pt film and hence its spin diffusion length (λ_{Pt}) is independent of t_{Pt} . Our work settles the controversy regarding the t_{Pt} dependence of λ_{Pt} by demonstrating its fundamental connection with ρ considered along the same direction of spin current flow.

DOI: [10.1103/PhysRevB.103.224403](https://doi.org/10.1103/PhysRevB.103.224403)

I. INTRODUCTION

Thin film bilayers comprised of a high spin-orbit coupling (SOC) metal and normal metal-ferromagnet (NM/FM) thin films are central to some of the most interesting phenomena in contemporary spintronics, such as spin pumping [1,2], the spin Hall effect (SHE) [3] and current-induced spin-orbit torques (SOTs) [4].

A key, and sometimes controversial, issue in current spintronics research is the correct quantification of the spin diffusion length (λ_s) in the NM, i.e., the characteristic length over which the spin current dissipates. For example, Pt, by far the most extensively studied material for the generation and detection of spin currents, λ_s , exhibits a large dispersion of values in the literature [5–10]. Moreover, the spin-flip scattering mechanisms that determine λ_s are not completely understood. It has been generally assumed that the Elliot-Yaffet (EY) mechanism is the dominant mechanism in Pt; however, recent results have shown that both the Dyakonov-Perel (DP) and EY spin relaxation mechanisms coexist at low temperatures [11].

The origin of the discrepancies in the reported values of λ_s may be related to *how* it has been measured. For example, estimation of λ_s has relied primarily on the measurement of inverse spin Hall effect (ISHE) voltage (V_{ISHE}) at FM/NM bilayers with variable NM thickness (t_{NM}) [5,8–10,12–16], or conversely, the detection of FM layer magnetization pertur-

bations due to the SHE generated spin currents in the NM layer [17–19]. Such *electrical detection methods* always rely on the spin-to-charge current conversion factor, the so-called spin Hall angle (θ_{SH}), to calculate λ_s . As an example, in FM/NM bilayers, V_{ISHE} has the form [10]

$$V_{\text{ISHE}} \propto \theta_{\text{SH}} \lambda_s, \quad (1)$$

which is valid for $t_{\text{NM}} \gg \lambda_s$. In Eq. (1), both θ_{SH} and λ_s have a dependence on the resistivity of the NM layer (ρ). On the one hand, there is a proportionality between θ_{SH} and ρ that is characteristic of the intrinsic Berry-phase-related mechanism of SHE, currently accepted to be dominant in Pt [18,20–24]. On the other hand, the connection of λ_s with ρ arises from its proportionality to the square root of the characteristic momentum relaxation time (τ_p), hence $\lambda_p \propto \rho^{-1/2}$ [18,25].

At this point, we emphasize a key detail that has not been addressed by previous works. If we assume $\theta_{\text{SH}} \propto \rho$, we expect ρ to correspond to the *in-plane* resistivity of the film (ρ_{\parallel}) given that the charge current flows in-plane. In a similar vein, if we have a spin current flowing out-of-plane of the FM layer, it is reasonable to expect that λ_s will then be determined by the *out-of-plane* resistivity (ρ_{\perp}) of NM. With this reasoning, an expression of the form $V_{\text{ISHE}} \propto \theta_{\text{SH}}(\rho_{\parallel}) \lambda_s(\rho_{\perp})$ should be employed to model the experimental data. Curiously, ρ_{\parallel} has been employed not only to account for the t_{NM} dependence of θ_{SH} but also for λ_s dependence assuming implicitly that $V_{\text{ISHE}} \propto \theta_{\text{SH}}(\rho_{\parallel}) \lambda_s(\rho_{\parallel})$. We should also consider that whereas ρ_{\perp} is similar to the bulk value and therefore independent of

*claudio.gonzalezfu@usm.cl

t_{NM} , ρ_{\parallel} is remarkably higher and exhibits a strong dependence on t_{NM} due to reduced dimensionality.

An alternative method to extract λ_s is with an experimental method that relies solely on the spin pumping effect and is therefore unaffected by the in-plane generated charge currents and the value of θ_{SH} . Analyzing the Gilbert damping (α) enhancement due to the NM layer in ferromagnetic resonance experiments accomplishes this goal. If we fix the thickness of the FM layer and vary t_{NM} , the extracted α versus t_{NM} will follow a characteristic exponential saturation curve [1,2,26]. Although this is a well-known technique, the precise quantification of λ_s requires a series of bilayers with a small to negligible interfacial spin memory loss (SML) [6,27], which is uncommon. Therefore, this requirement has difficult reliable quantification of λ_s , because if SML is included in the analysis, at least two additional adjustable parameters are required, namely the spin mixing conductance ($g^{\uparrow\downarrow}$) and the interfacial depolarization parameter (δ).

In this work, we aim to settle the issue of the t_{NM} dependence of λ_s in Pt by employing variable temperature spin pumping experiments and analyzing the Gilbert damping. The negligible SML of our samples provides us with the opportunity to perform an analysis that integrates the ρ versus T dependence of Pt into λ_s , and to test the diffusive model of Tserkovnyak *et al.* [1,2]. Our work provides strong evidence that ρ_{\perp} determines λ_s and hence it does not depend on t_{NM} . In addition, we show evidence of the low influence of temperature in τ_s of Pt, in agreement with recently reported results [11].

II. EXPERIMENTAL DETAILS

A series of NiFe(20 nm)/Pt(t_{Pt}) bilayers were deposited onto thermally oxidized SiO₂ substrates by dc magnetron sputtering, with $t_{\text{Pt}} = 1, 2, 4$ and 7 (all thicknesses expressed in nm). The Ar sputtering gas pressure and power during deposition was 1 mTorr and 60 W, respectively. To promote better uniformity, the substrates were rotated during growth. A NiFe(20 nm)/Ag(2 nm) reference sample was also deposited under the same conditions. As the reported value of λ_s for Ag is approximately 450 nm [28], we can confidently neglect spin attenuation effects in this reference sample. The samples were finally annealed *in situ* at 500 K for 1 h in vacuum. This procedure has been found to substantially improve the interfacial spin conductance, as evidenced by the onset of the characteristic $\Delta\alpha$ versus t_{NM} curve as compared to the nonannealed samples. Further details of this annealing study will be addressed in a future work.

Also, in order to check the good coverage of the NiFe by Pt overlayer in our samples, we have carried out scanning tunneling microscopy measurements of the $t_{\text{Pt}} = 7$ nm sample (Appendix B).

The thin film bilayer samples were characterized by broadband (6–16 GHz) ferromagnetic resonance at 100, 150, 200, and 293 K. The measurements are performed at a fixed frequency while sweeping the magnetic field through resonance. Due to the field-modulated measurement scheme, the derivative of the microwave absorption is recorded. The obtained resonance spectra are then fitted to the sum of a symmetric

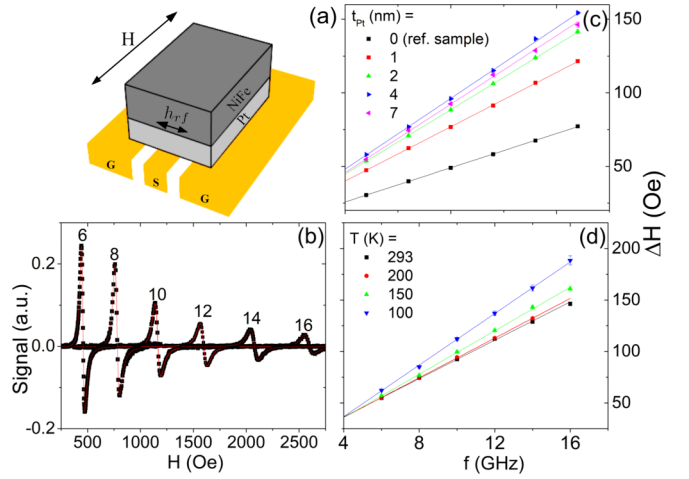


FIG. 1. (a) Schematic of the broadband measurement system, (b) FMR spectra of the NiFe(20 nm)/Pt(7 nm) film at 293 K for different values of f in GHz, (c) FMR peak linewidths vs f at room temperature for NiFe(20 nm)/Pt(t_{Pt}) for $t_{\text{Pt}} = 1, 2, 4$, and 7 nm and Ag capped reference sample and (d) ΔH vs f for NiFe(20 nm)/Pt(7 nm) film at $T = 100, 150, 200$ and 293 K. In (c) and (d) continuous lines are linear fittings to the experimental points.

and asymmetric Lorentzian function:

$$P = \frac{d}{dH} \left[\frac{S(\Delta H)^2 + A_S(H - H_r)}{4(H - H_r)^2 + (\Delta H)^2} \right], \quad (2)$$

where H_r , ΔH , S , and A_S are the fitting parameters corresponding to the resonance field, the linewidth, the symmetric, and the asymmetric components of the Lorentzian curve, respectively. The Gilbert damping was obtained by a linear fit of the frequency dependence of the extracted linewidth:

$$\Delta H = \Delta H_0 + \frac{2h\alpha f}{g\mu_B\mu_0}, \quad (3)$$

where ΔH_0 , μ_0 , μ_B , h , and g are the inhomogeneous broadening, vacuum permeability, Bohr magneton, Planck's constant, and gyromagnetic factor ($g = 2.11$ for NiFe [29]), respectively. Additional details of data analysis protocol can be found in Ref. [30]. Figure 1 shows representative graphs of these results.

III. RESULTS AND DISCUSSION

The NiFe/Pt bilayers show an increased α in comparison to the NiFe/Ag reference sample. This difference is due to the imbalance between the amount of angular momentum carried by the electron spins pumped into the NM, and the portion flowing back into the FM. The additional damping contribution, $\Delta\alpha$, was quantified by simply subtracting the damping of the Ag reference sample (α_0) from the damping of the NiFe/Pt bilayers, $\Delta\alpha = \alpha - \alpha_0$. We modeled the $\Delta\alpha$ versus t_{Pt} curves using the diffusive theory of spin pumping [1,2], in which the additional damping contribution ($\Delta\alpha$) of the NiFe/Pt bilayers is given by

$$\Delta\alpha = \alpha - \alpha_0 = \frac{g\mu_B g_{\text{eff}}^{\uparrow\downarrow}}{4\pi M_s t_{\text{F}}}, \quad g_{\text{eff}}^{\uparrow\downarrow} = \frac{g^{\uparrow\downarrow}}{1 + g^{\uparrow\downarrow}\beta}, \quad (4)$$

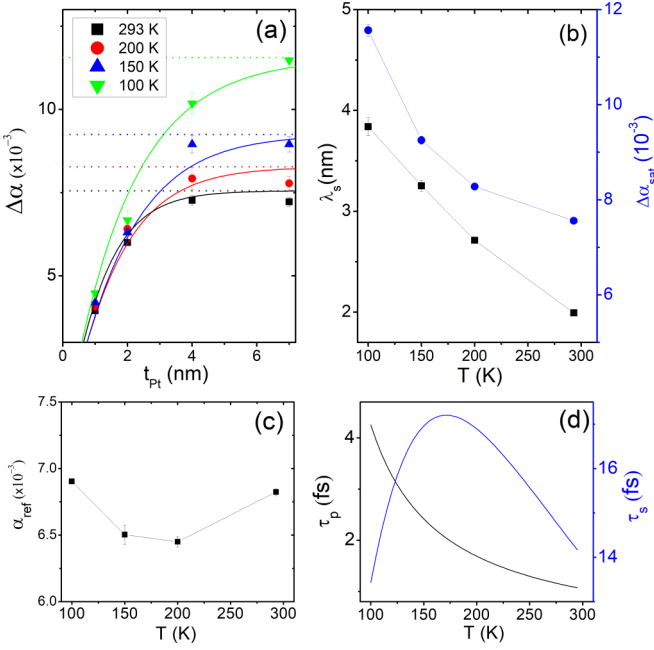


FIG. 2. (a) t_{Pt} -dependence of α for NiFe(20 nm)/Pt(t_{Pt}) bilayers at $T = 100, 150, 200,$ and 293 K. Symbols are the experimental data, and continuous lines are fitting to the EY-DP model employed in this work. Dotted horizontal lines are at corresponding values of $\Delta\alpha_{sat}$. (b) T -dependence of λ_s and $\Delta\alpha_{sat}$ obtained from the EY-DP model, (c) experimental T -dependence of α for Ag capped reference sample, and (d) T -dependence of τ_p , derived from Eq. (8), and τ_s derived from the EY-DP model.

where g , μ_B , M_s , and t_F are the gyromagnetic factor, Bohr magneton, saturation magnetization, and thickness of the ferromagnet, respectively. $g_{eff}^{\uparrow\downarrow}$ is the *effective* spin mixing conductance of the interface, defined in terms of the intrinsic spin mixing conductance $g^{\uparrow\downarrow}$ and the back-flow factor:

$$\beta = \frac{\tau_s \tanh^{-1}(t_{Pt}/\lambda_s)}{h\nu\lambda_s}, \quad (5)$$

where ν is the single spin density of states of NM. Note, α_0 does not show a significant dependence on temperature, as shown in Fig. 2.

λ_s can be expressed by the relation

$$\lambda_s = v_F \sqrt{\frac{\tau_s \tau_p}{3}}, \quad (6)$$

where v_F is the Fermi speed, and τ_s and τ_p are the characteristic spin and momentum relaxation times, respectively.

As explained in Appendix A, SML [6,27,31] can be neglected in our samples. The saturation value of $\Delta\alpha$ is defined as $t_{NM} \rightarrow \infty$

$$\Delta\alpha_{sat} = \frac{g\mu_B g^{\uparrow\downarrow}}{4\pi M_s t_F} \left(1 + \frac{g^{\uparrow\downarrow}}{h\nu v_F} \times \sqrt{\frac{3\tau_s}{\tau_p}} \right)^{-1}. \quad (7)$$

From a physical point of view, the positive correlation of $\Delta\alpha_{sat}$ with τ_p arises from the increment of the diffusion coefficient $D = \lambda_s^2/\tau_s$ [1] of the spin polarized electrons in the NM layer. This effect overcomes the negative correlation between $\Delta\alpha_{sat}$ and τ_p arising from the enhancement of λ_s and the concurrent

increase of spin current backflow. Overall, this translates into an increment of $\Delta\alpha_{sat}$ as T goes down.

Regarding the correlation between τ_p and τ_s , there have been two mechanisms proposed for spin-flip scattering: Elliott-Yaffet [32,33] (EY) and Dyakonov-Perel [34,35] (DP). In the EY picture, each momentum scattering event has a probability of being a spin-flip event ($\tau_s \propto \tau_p$), whereas in the DP picture, the spin dephasing occurs continuously, so $\tau_s \propto \tau_p^{-1}$.

The temperature variation of $\Delta\alpha_{sat}$ provides valuable insight into the physics of the various scattering mechanisms in Pt, since $\tau_p \propto \rho^{-1}$ and ρ increases in an approximately linear manner with temperature over the range of temperatures studied here. If, for example, we assume the EY model alone is valid, according to Eq. (6), λ_s should decrease with increasing temperature, in agreement with previous predictions and observations [11,18,36]. In this framework, according to Eq. (7), $\Delta\alpha_{sat}$ should be independent of temperature due to the cancellation of τ_p on the right side of the equation. This clearly contradicts our experimental results: in Fig. 2(a), a twofold increase of $\Delta\alpha_{sat}$ in the temperature range from 100 to 293 K is observed. On the other side, if we assume the DP model is the exclusive spin-flip scattering mechanism, it leads to the unacceptable outcome that λ_s is independent of temperature, in this case from the cancellation of τ_p on the right side of Eq. (6). This model, however, is consistent with our observation of increasing $\Delta\alpha_{sat}$ as T decreases predicted by Eq. (7).

Note that these conclusions are still valid for models that also include SML at the interface [6,27,37], despite the fact that SML narrows the range of variation of $g_{eff}^{\uparrow\downarrow}$ versus t_{NM} .

Although it is generally accepted that EY should be the dominant mechanism of spin-flip scattering in crystal systems with cubic symmetry, the evidence is not conclusive. For example, recently evidence of dominant DP [31,38] and partial contributions of both DP and EY mechanisms [38–40] in polycrystalline Pt films have been found. Boone *et al.* [31] performed an extensive analysis of spin pumping in NiFe/Pt and NiFe/Pd bilayers and found that their data are better modeled by a DP model. Villamor *et al.* found significant deviations from the EY mechanism in Cu [41]. Very recently, Freeman *et al.* [11] found evidence of the DP mechanism in Pt at cryogenic temperatures. The authors interpreted their results as a near compensation of the DP and EY mechanisms for a broad range of temperatures, such that τ_s varies only 20% from 50 K to room temperature. Coincidentally, our results suggest that a mixed or intermediate model between DP and EY can account for our qualitative observations.

To test this hypothesis, we modeled τ_p in Eq. (7) using the Sommerfeld model:

$$\tau_p = 3(q_e^2 \nu v_F^2 \rho)^{-1}. \quad (8)$$

Here, in contrast to other works [11,31], we have chosen not to utilize the Drude approximation since it assumes a spherical Fermi surface of Pt, which is an oversimplification and inadequate approximation [42].

We can narrow the possible range of variation of ρ by using Eqs. (7) and (8) in a given range of variation of $\Delta\alpha_{sat}$ even without knowing the explicit value of $\rho(T)$. Defining ρ_{100} , ρ_{293} , $\Delta\alpha_{sat,100}$, and $\Delta\alpha_{sat,293}$ as the values of resistivity

and $\Delta\alpha_{\text{sat}}$ at 100 and 293 K, respectively, we can derive the following inequality from Eq. (7):

$$\left(\frac{\Delta\alpha_{\text{sat},100}}{\Delta\alpha_{\text{sat},293}}\right)^2 \leq \frac{\rho_{293}}{\rho_{100}}. \quad (9)$$

Central to this work is the question of which resistivity, i.e., in-plane ρ_{\parallel} or out-of-plane ρ_{\perp} , determines λ_s .

Apart from the strong thickness dependence of ρ_{\parallel} , a key difference with respect to ρ_{\perp} is the temperature dependence. The T -variation of ρ_{\parallel} is weaker than ρ_{\perp} , which is mainly due to the strong contribution of the temperature-independent scattering mechanisms such as electron-surface and electron grain-boundary, in comparison to the electron-phonon scattering that tends to be dominant in bulk films at temperatures higher than 50 K [43,44]. In particular, for bulk Pt, the reported temperature ratio ρ_{293}/ρ_{100} is approximately 3.6 [45,46], while for ρ_{\parallel} it is only up to 1.5 in 20-nm-thick sputtered samples [21]. Given that the T -dependence of ρ_{\parallel} decreases with decreasing t_{NM} [47,48], ρ_{293}/ρ_{100} must be even smaller in our films. We experimentally obtained a value of $(\Delta\alpha_{\text{sat},100}/\Delta\alpha_{\text{sat},293})^2 \sim 2.25$, which sets a lower limit to ρ_{293}/ρ_{100} . Consequently, the commonly accepted assumption that ρ_{\parallel} determines λ_s is hardly reconcilable with our experimental observations.

The assumption of a dominant EY mechanism in τ_s would reduce the possible range of variation of $\Delta\alpha_{\text{sat}}$ across temperature, due to the τ_p/τ_s ratio of the backflow factor in Eq. (7). Consequently, we would need to increase the lower possible limit of ρ_{293}/ρ_{100} to compensate for the former effect in order to be compatible with our experimental results. The same thing would happen if we included SML in our analysis, given that this effect always reduces the influence of the spin-current backflow over the value of $\Delta\alpha_{\text{sat}}$ [27], which is ultimately the origin of the α_{sat} variation across temperature. In summary, we conclude that λ_s has to be determined by ρ_{\perp} instead of ρ_{\parallel} . Furthermore, in our analysis, a greater contribution of the EY mechanism or SML would strengthen this conclusion.

Our experimental data points are then fit assuming ρ_{\perp} in Eq. (8) as the total resistivity of our system, equivalent to the bulk resistivity of Pt [45]. The value of $\mu_0 M_s = 0.94 \pm 0.05$ T was extracted from the FMR measurements. $\nu = 1.1 \times 10^{48}$ J⁻¹m⁻³ and $v_F = 8.8 \times 10^5$ m/s were taken from Refs. [49] and [50], respectively. We modeled the spin relaxation in Pt as a superposition of the EY and DP mechanisms [11] (EY-DP model): $\tau_s^{-1} = \tau_{\text{EY}}^{-1} + \tau_{\text{DP}}^{-1}$, where $\tau_{\text{EY}} = c_{\text{EY}}\tau_p$ and $\tau_{\text{DP}} = c_{\text{DP}}\tau_p^{-1}$ are the characteristic spin relaxation times associated with EY and DP mechanisms, respectively. The coefficients c_{EY} and c_{DP} are the parameters to model their effective strengths. They, in combination with $g_{\uparrow\downarrow}$, were the set of adjustable parameters for the fitting of all the experimental data. The results were $g_{\uparrow\downarrow} = (2.26 \pm 0.06) \times 10^{20}$ m⁻², $c_{\text{EY}} = 16.8 \pm 0.3$, and $c_{\text{DP}} = (7.03 \pm 0.06)$ s², with $R^2 = 0.9976$ for the fit. The fitted curves are shown in Fig. 2(a) and the corresponding values of λ_{Pt} and $\Delta\alpha_{\text{sat}}$ are found in Fig. 2(b), whereas the expected temperature dependence of τ_p according to Eq. (8) and τ_s according to the EY-DP model are shown in Fig. 2(d). The excellent agreement of our predictions with the experimental data is remarkable given the simplicity of our assumptions. The connection between ρ_{\perp} and bulk resistivity is also in agreement with structural analysis of the $t_{\text{Pt}} = 7$ nm sample, as shown in Appendix B.

Our results are robust since spin pumping experiments based on the Gilbert damping are not affected by the value of θ_{SH} or ρ_{\parallel} . Consequently, many of the potential problems that can influence measurements based on electrical detection are simply not present here. This offers a new perspective to the discussion that appeared recently regarding the thickness dependence of ρ_{\parallel} and its influence on λ_s . In particular, it has been proposed that neglecting this dependence may promote the large spread of λ_s values present in the literature [18,25,51]. Consequently, many recent works explicitly consider a thickness-dependent λ_s [18,25,43,51–53].

We believe that this mistake arises in great part because, whereas λ_s is determined by ρ_{\perp} and θ_{SH} is determined by ρ_{\parallel} , both ρ_{\perp} and ρ_{\parallel} have been treated *indistinctly*.

A further confirmation of our hypothesis arises when we review the published values of λ_{Pt} in works that obtain it from the $\alpha(t_{\text{Pt}})$ curve and in bilayers with small SML. The dispersion of λ_s values in works that satisfy these criteria [51,54–56] is from 1.6 to 1.8 nm at room temperature (including the present work). Analogously, the published values of λ_s of Pd applying the same selection criteria range from 6 to 9 nm [26,54,57]. Generally, the values of λ_s obtained by spin pumping experiments are more consistent for a given material as compared to those found by electrical detection methods. An additional check of the consistency of the t_{NM} -independent hypothesis can be found in the recent work of Swindells *et al.* [51], on which the authors reported values of λ_{Pt} obtained by spin pumping enhanced α , in a series of bilayers consisting on Pt in combination with different FM materials. The work shows a direct comparison of the fitted value of λ_{Pt} with t_{NM} -dependent and t_{NM} -independent expressions. In the second case, the values of λ_{Pt} were fairly more similar among the systems studied, rounding 1.6 nm in all cases. In comparison, t_{NM} -dependent fitting gave a variation between 6.6 and 9.5 nm for bulk λ_{Pt} .

Our findings also make us discard a hypothesis of spin relaxation in Pt based on DP or EY mechanisms acting alone. A similar finding was reported in Ref. [11], and as in our work, they find that the T variation of τ_s is much smaller than τ_p . In that work, the existence of the DP mechanism in Pt was supported also with evidence from magnetoresistance measurements. However, a theoretical explanation of how this could exist in the centrosymmetric fcc structure of Pt is not present. Another option may be an intermediate spin relaxation regime between EY and DP rather than a mixed one. A recent work [58] has proposed that the characteristic relations $\tau_s \propto \tau_p$ from EY and $\tau_s \propto \tau_p^{-1}$ from DP spin relaxation mechanisms are the limit cases of a broad spectrum of spin relaxations regimes. Along these lines, the unexpectedly small *effective* correlation between τ_s and τ_p observed in this work and in Ref. [11] would mean simply that an intermediate relation ($\tau_s \propto \tau_p^0$) is at least more appropriate to describe the actual spin relaxation in Pt. We expect that our results will motivate further theoretical investigations in this respect.

IV. CONCLUSIONS

In summary, we have shown via temperature-dependent spin pumping experiments that, in the framework of the

diffusion theory, the spin diffusion length is determined by the out-of-plane resistivity of the NM layer and hence it is not dependent on its thickness. Our results also support the recent findings showing the impossibility to explain τ_s of Pt exclusively by EY or DP mechanisms, suggesting a mixed or intermediate spin relaxation regime between them.

We believe that the apparent controversy regarding the different values of λ_s found in SHE experiments must be due to the t_{NM} dependence of θ_{SH} rather than the t_{NM} dependence of λ_s . The first is proportional to ρ_{\parallel} and hence very variable with fabrication conditions, whereas the second depends on ρ_{\perp} , which is close to bulk resistivity, independently of t_{NM} .

ACKNOWLEDGMENTS

This work was supported by FONDECYT Grant No. 3170908, ANID FONDECYT/REGULAR 1201102, ANID PIA/APOYO AFB180002, ANID FONDEQUIP EQM140161, and European Union's Horizon 2020 research and innovation program under the Marie Skłodowska-Curie Grant Agreement No. 645658 (DAFNEOX Project).

APPENDIX A: NEGLIGIBLE SPIN MEMORY LOSS IN NiFe/Pt BILAYERS

We confirmed the negligible interface spin memory loss (SML) in our samples comparing the extrapolated value of Gilbert's damping α at $t_{\text{Pt}} \rightarrow 0$, namely $\alpha_{t_{\text{Pt}} \rightarrow 0}$, and the measured value of α of the reference sample (α_{ref}). It should be noted that due to the extra damping generated by the normal metal, $\Delta\alpha(t_{\text{NM}})$ is nonzero at $t_{\text{NM}} = 0$ in all the models that consider finite SML [6,27,31,37,59,60], and its value is often comparable to $\Delta\alpha(t_{\text{NM}} \rightarrow \infty)$ [27,61].

To get $\alpha_{t_{\text{Pt}} \rightarrow 0}$ we employed the following extrapolation function to fit the α versus t_{Pt} curve at room temperature (Fig. 3):

$$\alpha(t_{\text{Pt}}) = \alpha_{t_{\text{Pt}} \rightarrow 0} + \alpha_s \exp\left(\frac{-t_{\text{Pt}}}{t_{\text{sat}}}\right), \quad (\text{A1})$$

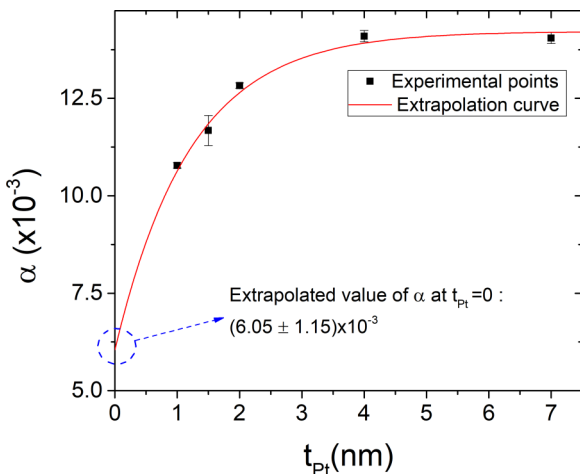


FIG. 3. α vs t_{Pt} curve at room temperature (293 K) for the NiFe(20 nm)/Pt(t_{Pt}) series of samples (black squares) and SML extrapolation curve (red continuous line).

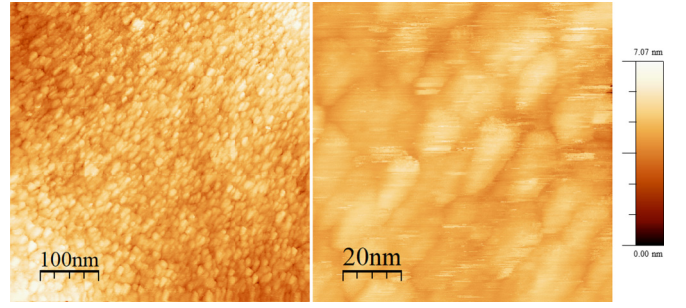


FIG. 4. Representative STM images of the $t_{\text{Pt}} = 12$ nm sample at two different amplifications.

where $\alpha_{t \rightarrow 0}$, t_{sat} , α_s are the fitting parameters. The obtained value of $\alpha_{t_{\text{Pt}} \rightarrow 0}$ was $(6.05 \pm 1.5) \times 10^{-3}$, which is below the value of the reference sample: $\alpha_{\text{ref}} = (6.8 \pm 0.1) \times 10^{-3}$, but inside the fitting uncertainty margin.

We emphasize that we do not give any physical meaning to α_s nor t_{sat} in (A1), as they are only for extrapolation purposes. In this sense, our method is analogous to other extrapolation methods employed for quantifying interfacial magnetic effects such as the proximity effect [62] or the interfacial perpendicular anisotropy energy density [63].

APPENDIX B: SCANNING TUNNELING MICROSCOPY STUDY

The surface of the $t_{\text{Pt}} = 7$ nm sample was characterized by scanning tunneling microscopy (STM, Omicron VT SPM) in ultrahigh vacuum (pressure below 10^{-8} Torr) at room temperature. Tips were made from Pt/Ir wire, and checked by imaging the HOPG surface with atomic resolution. Images were analyzed with WSXM software [64], and representative examples are shown in Fig. 4. In that figure, it can be observed that the film is continuous and the typical grain lateral size is of the same order as the thickness of the film. Therefore, we do not expect significant grain boundary scattering for electrons moving along the out-of-plane direction.

Eventual interface discontinuities in smaller t_{Pt} samples could imply that the actual value of ρ_{\perp} differs slightly from bulk Pt resistivity due to a reduced effective area of conduction. However, even in this scenario, our conclusions would be unaltered since our analysis relies on the *relative* variation of ρ_{\perp} across T and not on its *absolute* value: our observations are explainable if and only if the ρ that determines λ_s exhibits *bulklike* behavior with respect to T . The latter is not modified by a reduced area of conduction, despite the fact that the actual value of ρ_{\perp} is. Interface discontinuities could also affect the areal density of channels available for spin transport, and this must be reflected in the value of $g^{\uparrow\downarrow}$. However, this is a fitted parameter that does not influence the other aspects of our analysis. The evident trends of variation of $\Delta\alpha_{\text{sat}}$ and λ_s with respect to T in Fig. 2(a) support our qualitative conclusions, independent of the specific value of $g^{\uparrow\downarrow}$ or τ_s .

- [1] Y. Tserkovnyak, A. Brataas, and G. E. W. Bauer, *Phys. Rev. B* **66**, 224403 (2002).
- [2] Y. Tserkovnyak, A. Brataas, G. E. W. Bauer, and B. I. Halperin, *Rev. Mod. Phys.* **77**, 1375 (2005).
- [3] E. Saitoh, M. Ueda, H. Miyajima, and G. Tatara, *Appl. Phys. Lett.* **88**, 182509 (2006).
- [4] A. Manchon, J. Železný, I. M. Miron, T. Jungwirth, J. Sinova, A. Thiaville, K. Garello, and P. Gambardella, *Rev. Mod. Phys.* **91**, 035004 (2019).
- [5] V. Vlaminck, J. E. Pearson, S. D. Bader, and A. Hoffmann, *Phys. Rev. B* **88**, 064414 (2013).
- [6] Y. Liu, Z. Yuan, R. J. H. Wesselink, A. A. Starikov, and P. J. Kelly, *Phys. Rev. Lett.* **113**, 207202 (2014).
- [7] L. Bai, P. Hyde, Y. S. Gui, C.-M. Hu, V. Vlaminck, J. E. Pearson, S. D. Bader, and A. Hoffmann, *Phys. Rev. Lett.* **111**, 217602 (2013).
- [8] K. Kondou, H. Sukegawa, S. Mitani, K. Tsukagoshi, and S. Kasai, *Appl. Phys. Express* **5**, 073002 (2012).
- [9] A. Azevedo, L. H. Vilela-Leão, R. L. Rodríguez-Suárez, A. F. Lacerda Santos, and S. M. Rezende, *Phys. Rev. B* **83**, 144402 (2011).
- [10] K. Ando, S. Takahashi, J. Ieda, Y. Kajiwara, H. Nakayama, T. Yoshino, K. Harii, Y. Fujikawa, M. Matsuo, S. Maekawa, and E. Saitoh, *J. Appl. Phys.* **109**, 103913 (2011).
- [11] R. Freeman, A. Zholid, Z. Dun, H. Zhou, and S. Urazhdin, *Phys. Rev. Lett.* **120**, 067204 (2018).
- [12] O. Mosendz, V. Vlaminck, J. E. Pearson, F. Y. Fradin, G. E. W. Bauer, S. D. Bader, and A. Hoffmann, *Phys. Rev. B* **82**, 214403 (2010).
- [13] L. Liu, T. Moriyama, D. C. Ralph, and R. A. Buhrman, *Phys. Rev. Lett.* **106**, 036601 (2011).
- [14] Z. Feng, J. Hu, L. Sun, B. You, D. Wu, J. Du, W. Zhang, A. Hu, Y. Yang, D. M. Tang, B. S. Zhang, and H. F. Ding, *Phys. Rev. B* **85**, 214423 (2012).
- [15] H. Nakayama, K. Ando, K. Harii, T. Yoshino, R. Takahashi, Y. Kajiwara, K. Uchida, Y. Fujikawa, and E. Saitoh, *Phys. Rev. B* **85**, 144408 (2012).
- [16] J. E. Gómez, B. Zerai Tedlla, N. R. Álvarez, G. Alejandro, E. Goovaerts, and A. Butera, *Phys. Rev. B* **90**, 184401 (2014).
- [17] Q. Hao and G. Xiao, *Phys. Rev. Appl.* **3**, 034009 (2015).
- [18] M.-H. Nguyen, D. C. Ralph, and R. A. Buhrman, *Phys. Rev. Lett.* **116**, 126601 (2016).
- [19] Y. Du, H. Gamou, S. Takahashi, S. Karube, M. Kohda, and J. Nitta, *Phys. Rev. Appl.* **13**, 054014 (2020).
- [20] G. Y. Guo, S. Murakami, T.-W. Chen, and N. Nagaosa, *Phys. Rev. Lett.* **100**, 096401 (2008).
- [21] E. Sagasta, Y. Omori, M. Isasa, M. Gradhand, L. E. Hueso, Y. Niimi, Y. C. Otani, and F. Casanova, *Phys. Rev. B* **94**, 060412(R) (2016).
- [22] M. Isasa, E. Villamor, L. E. Hueso, M. Gradhand, and F. Casanova, *Phys. Rev. B* **91**, 024402 (2015).
- [23] M. Morota, Y. Niimi, K. Ohnishi, D. H. Wei, T. Tanaka, H. Kontani, T. Kimura, and Y. Otani, *Phys. Rev. B* **83**, 174405 (2011).
- [24] L. Zhu, L. Zhu, M. Sui, D. C. Ralph, and R. A. Buhrman, *Sci. Adv.* **5**, eaav8025 (2019).
- [25] K. Roy, *Phys. Rev. B* **96**, 174432 (2017).
- [26] J. Foros, G. Woltersdorf, B. Heinrich, and A. Brataas, *J. Appl. Phys.* **97**, 10A714 (2005).
- [27] J.-C. Rojas-Sánchez, N. Reyren, P. Laczkowski, W. Savero, J.-P. Attané, C. Deranlot, M. Jamet, J.-M. George, L. Vila, and H. Jaffrès, *Phys. Rev. Lett.* **112**, 106602 (2014).
- [28] M. Isasa, E. Villamor, L. Fallarino, O. Idigoras, A. K. Suszka, C. Tollan, A. Berger, L. E. Hueso, and F. Casanova, *J. Phys. D* **48**, 215003 (2015).
- [29] J. M. Shaw, H. T. Nembach, T. J. Silva, and C. T. Boone, *J. Appl. Phys.* **114**, 243906 (2013).
- [30] C. Gonzalez-Fuentes, R. K. Dumas, and C. García, *J. Appl. Phys.* **123**, 023901 (2018).
- [31] C. T. Boone, J. M. Shaw, H. T. Nembach, and T. J. Silva, *J. Appl. Phys.* **117**, 223910 (2015).
- [32] R. J. Elliott, *Phys. Rev.* **96**, 266 (1954).
- [33] Y. Yafet, *Phys. Lett. A* **98**, 287 (1983).
- [34] M. I. D'yakonov and V. I. Perel', *Sov. Phys. JETP Lett.* **13**, 467 (1971).
- [35] M. D. Mower, G. Vignale, and I. V. Tokatly, *Phys. Rev. B* **83**, 155205 (2011).
- [36] Y. Liu, Z. Yuan, R. J. H. Wesselink, A. A. Starikov, M. van Schilfgaarde, and P. J. Kelly, *Phys. Rev. B* **91**, 220405(R) (2015).
- [37] X. Tao, Q. Liu, B. Miao, R. Yu, Z. Feng, L. Sun, B. You, J. Du, K. Chen, S. Zhang, L. Zhang, Z. Yuan, D. Wu, and H. Ding, *Sci. Adv.* **4**, eaat1670 (2018).
- [38] J. Ryu, M. Kohda, and J. Nitta, *Phys. Rev. Lett.* **116**, 256802 (2016).
- [39] Y. Dai, S. J. Xu, S. W. Chen, X. L. Fan, D. Z. Yang, D. S. Xue, D. S. Song, J. Zhu, S. M. Zhou, and X. Qiu, *Phys. Rev. B* **100**, 064404 (2019).
- [40] N. H. Long, P. Mavropoulos, D. S. G. Bauer, B. Zimmermann, Y. Mokrousov, and S. Blügel, *Phys. Rev. B* **94**, 180406(R) (2016).
- [41] E. Villamor, M. Isasa, L. E. Hueso, and F. Casanova, *Phys. Rev. B* **87**, 094417 (2013).
- [42] D. H. Dye, J. B. Ketterson, and G. W. Crabtree, *J. Low Temp. Phys.* **30**, 813 (1978).
- [43] E. Montoya, P. Omelchenko, C. Coutts, N. R. Lee-Hone, R. Hübner, D. Broun, B. Heinrich, and E. Girt, *Phys. Rev. B* **94**, 054416 (2016).
- [44] G. Kästle, H.-G. Boyen, A. Schröder, A. Plettl, and P. Ziemann, *Phys. Rev. B* **70**, 165414 (2004).
- [45] D. B. Poker and C. E. Klabunde, *Phys. Rev. B* **26**, 7012 (1982).
- [46] J. W. Arblaster, *Johnson Matthey Technol. Rev.* **59**, 174 (2015).
- [47] J. S. Agustsson, U. B. Arnalds, A. S. Ingason, K. B. Gylfason, K. Johnsen, S. Olafsson, and J. T. Gudmundsson, *J. Phys.: Conf. Ser.* **100**, 082006 (2008).
- [48] R. Henriquez, R. Roco, S. Bravo, V. Del Campo, C. Gonzalez-Fuentes, S. Donoso, and P. Häberle, *Appl. Surf. Sci.* **489**, 403 (2019).
- [49] H. J. Jiao and G. E. W. Bauer, *Phys. Rev. Lett.* **110**, 217602 (2013).
- [50] J. B. Ketterson and L. R. Windmiller, *Phys. Rev. B* **2**, 4813 (1970).
- [51] C. Swindells, A. T. Hindmarch, A. J. Gallant, and D. Atkinson, *Phys. Rev. B* **99**, 064406 (2019).
- [52] L. Zhu, D. C. Ralph, and R. A. Buhrman, *Phys. Rev. Appl.* **10**, 031001(R) (2018).
- [53] Y. Ou, S. Shi, D. C. Ralph, and R. A. Buhrman, *Phys. Rev. B* **93**, 220405(R) (2016).

- [54] M. Caminale, A. Ghosh, S. Auffret, U. Ebels, K. Ollefs, F. Wilhelm, A. Rogalev, and W. E. Bailey, *Phys. Rev. B* **94**, 014414 (2016).
- [55] Y. Huo, F. L. Zeng, C. Zhou, and Y. Z. Wu, *AIP Adv.* **7**, 056024 (2017).
- [56] M. Belmeguenai, K. Aitoukaci, F. Zighem, M. S. Gabor, T. Petrisor, R. B. Mos, and C. Tiusan, *J. Appl. Phys.* **123**, 113905 (2018).
- [57] A. Kumar, S. Akansel, H. Stopfel, M. Fazlali, J. Åkerman, R. Brucas, and P. Svedlindh, *Phys. Rev. B* **95**, 064406 (2017).
- [58] P. Boross, B. Dóra, A. Kiss, and F. Simon, *Sci. Rep.* **3**, 3233 (2013).
- [59] K. Chen and S. Zhang, *Phys. Rev. Lett.* **114**, 126602 (2015).
- [60] K. Chen and S. Zhang, *IEEE Magn. Lett.* **6**, 1 (2015).
- [61] S. Azzawi, A. Ganguly, M. Tokaç, R. M. Rowan-Robinson, J. Sinha, A. T. Hindmarch, A. Barman, and D. Atkinson, *Phys. Rev. B* **93**, 054402 (2016).
- [62] K. A. Thórarinsdóttir, H. Palonen, G. K. Palsson, B. Hjörvarsson, and F. Magnus, *Phys. Rev. Materials* **3**, 054409 (2019).
- [63] S. Ikeda, K. Miura, H. Yamamoto, K. Mizunuma, H. D. Gan, M. Endo, S. Kanai, J. Hayakawa, F. Matsukura, and H. Ohno, *Nat. Mater.* **9**, 721 (2010).
- [64] I. Horcas, R. Fernández, J. M. Gómez-Rodríguez, J. Colchero, J. Gómez-Herrero, and A. M. Baro, *Rev. Sci. Instrum.* **78**, 013705 (2007).

Correction: The omission of a project number in the Acknowledgments has been fixed.